Solvent-Free, Solid State Processed Tapes of UHMWPE: Influence of Molar Mass and Molar Mass Distribution on Tensile Properties

Sanjay Rastogi[1,2,3], Dario Romano[1], Sara Ronca[1], Giuseppe Forte[1], Yefeng Yao[4], Niek Tops[2]
[1]Department of Materials, Loughborough University, Leicestershire, England (UK); [2]Research Institute, Teijin Aramid B.V., Arnhem, The Netherlands; [3]Materials Science, Maastricht University, Maastricht, The Netherlands; [4]Shanghai Key Laboratory of Magnetic Resonance, East China Normal University, Shanghai, China
sanjay.rastogi@teijinaramid.com; s.rastogi@lboro.ac.uk; sanjay.rastogi@maastrichtuniversity.nl

SUMMARY

In normal practice, ease in processing comes at the expense of reduction in mechanical properties. Here we show that by controlled synthesis, it is possible to synthesize a wide range of linear Ultra High Molecular Weight Polyethylenes that can be stretched uniaxially into tapes. In these uniaxially drawn tapes the bundles of fibres align themselves in a preferred crystal plane orientation accounting for an extraordinary high tensile modulus. The stretching process is accomplished in the solid state, without any solvent requirement. The ease in processing combined with controlled synthesis provides a unique opportunity to follow the influence of molar mass on mechanical properties.

INTRODUCTION

Recently, we have shown that making use of a single-site catalytic system it is possible to control entangled state in a semi-crystalline UHMWPE, having number average molar mass greater than a million g/mol, which can be drawn more than 200 times in solid state below the equilibrium melting temperature (~142 ^{o}C) of linear polyethylene[1-10]. The high deformation ratio of the compressed nascent reactor powder results into tapes having tensile modulus approaching 200 GPa and tensile strength 4.0 GPa.[3] For the synthesis, in our laboratory, two single site catalytic systems, Fujita FI catalyst having titanium as the metallic centre (Figure 1a)[6] and Enders catalyst having chromium as the metallic centre (Figure 1b)[13], have been identified. The synthesis predominantly done in the homogeneous condition, in the presence of a solvent or solvent mixture, can be translated to heterogenous support where the support used can vary from nanoparticles to elongated wires for example carbon nanotubes[4]. This process not only provides homogeneous mixing of nanoparticles (or functionalities) in the intractable polymer matrix, but also offers possibilities of upscaling requirements for commercial purposes. The principles adopted for controlling the entanglement density, during synthesis, are mainly control of the polymerization and crystallization kinetics – earlier proposed by Smith et al while using a Vanadium catalyst[11].

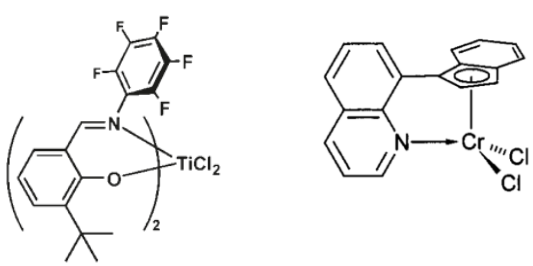

Figure 1: (a) Fujita catalyst with Titanium metallic center and (b) Enders catalyst with Chromium metallic center.

Characterization of Entangled State

To follow differences in the topological constraints, in the amorphous region of the semi-crystalline polymer and there influence on the resultant melt, solid state NMR, DSC and rheological studies have been performed. What follows is a brief overview of salient findings that have been of relevance in molecular understanding of the synthesised polymer.

Influence of Entanglements on Segmental Mobility of the Noncrystalline Region: To have insight on the entangled state of the polymer solid state NMR studies have been performed. Differences in the entangled and disentangled state become evident by following the chain diffusion of methylene segments from amorphous to crystalline regions. For the purpose use of ^{13}C NMR is made where the pulse sequence is tailored in a way to differentiate between the mobile and rigid components of the amorphous (or non-crystalline) and crystalline regions. For details the readers are requested to follow the references 5,7. Figure 2 highlights differences in the NMR spectra of the entangled and disentangled UHMWPE, synthesised using a conventional Z-N and single-site catalytic system, respectively.

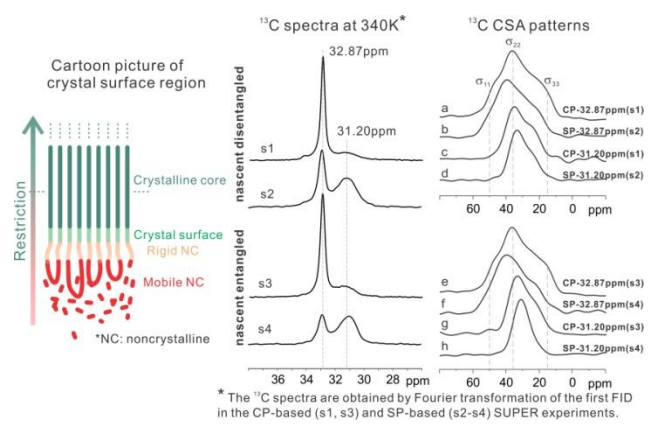

Figure 2: Left: schematic of crystal describing gradual transition of the geometrical restriction present in the sample; Middle: the ^{13}C spectra of the nascent disentangled and entangled samples obtained by Fourier transformation experiments: s1 and s3 are from the CP-based SUPER experiments of the disentangled and entangled samples; s2 and s4 are from the SP-based SUPER experiments of the disentangled and entangled samples, respectively. Right: the ^{13}C chemical shift anisotropy (CSA) powder patterns of the two nascent UHMWPEs

Melting Kinetics: In a series of publications we have also shown that melting behaviour of crystalline component strongly depends on entangled state of the amorphous region.[2,6,10] To recall, polymer melting that involves detachment of chains from crystal surface and their reeling

in melt can occur either by consecutive detachment or in cluster, the latter involving more than seven chain segments. During slow heating or annealing at the onset of the melting temperature, the cluster melting is observed in the crystals having entangled amorphous region whereas consecutive detachment of chains is observed in disentangled polyethylene. The two different melting processes of the crystalline zones that are dependent on the chain topology in the amorphous region, become evident by following the kinetics involved in the change in the ratio of the low and high melting temperature peaks, where the former is associated with the melt crystallised component arising on crystallization of the molten part whereas the high melting temperature peak is related with the remainder of the nascent component that did not melt on annealing. The rate at which the high temperature peak transforms into the low temperature peak is related with the entanglement density and molar mass. Figure 3, reproduced from reference 6 shows an example of melting kinetics related to the entangled state of the polymer.

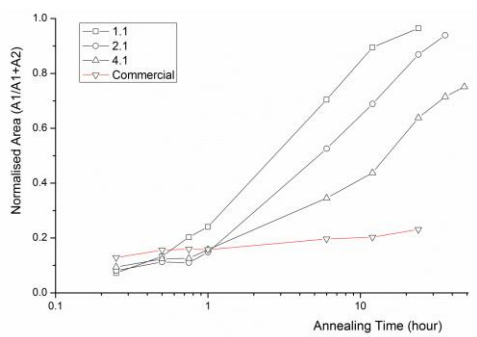

Figure 3: Evolution of the normalised area as a function of time for the synthesised polymers at three different pressures; unfilled squares, 1.1 atm (Mw ~9.9 x 10^6 g/mol; Mw/Mn ~ 2.6); unfilled circles, 2.1 atm (Mw ~15.3 x 10^6 g/mol; Mw/Mn ~ 3.0); unfilled up-triangles, 4.1 atm (Mw ~34.0 x 10^6 g/mol; Mw/Mn ~ 7.1); unfilled down-triangles, refers to a commercial Sigma-Aldrich UHMWPE for comparison.

Solid state deformation (biaxial): The disentangled UHMWPE provides opportunity to deform the compressed nascent powder not only uniaxially but also biaxillay, where the former can be used for applications in hard ballistics while the latter in membranes required for Lithium ion batteries or water purification or gas permeability and other demanding applications that require high isotropic high tensile and high modulus flexible films having thickness in the order of several microns. An example of the same is given in Figure 4.

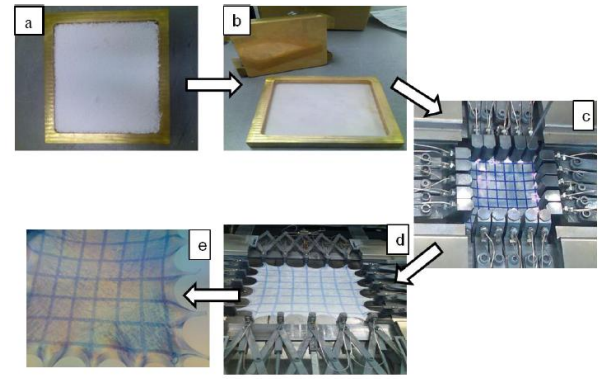

Figure 4: The figure shows biaxial deformation of compressed nascent powder. The powder depicted in figure a is compressed to make a film having thickness 225 microns shown in figure b. The film is mounted on Brukner biaxial machine and stretched 10 x 10 times, below the equilibrium melting point to get a film having metallic sound of several microns thickness. The film thus drawn, from the sample having molar mass 8 million g/mol, shows isotropic tensile strength in the region of 0.5 – 0.7 GPa. Permeability of the film can be varied by adding functionality such as hydroxyapatite or carbon nanotube or ethylene copolymer or graphene in the polymerization medium prior to the synthesis of disentangled UHMWPE. This route provides homogeneous dispersion of functionality in the intractable matrix of UHMWPE. Such a possibility is shown in the following section.

REFERENCES

[1] Rastogi, S., Lippits, D., Peters, G.W.M., Graf, R., Yao, Y., Spiess; H.W. *Nature Materials*, 4, 2005: 635-641.

[2] Lippits, D.R., Rastogi, S., Hohne, G.W., *Physical Review Letters*, 96, 2006: 218303-218307.

[3] Rastogi, S., Yao, Y., Ronca, S., Bos, J., Van der Eeem, *J. Macromolecules*, 44, 2011: 5558-5568.

[4] Andablo-Reyes, E.A., De Boer, E., Romano, D., Rastogi, S. *Journal of Rheology*, 58 (6), 2014: 1981-1986.

[5] Yao, Y., Jiang, S., Rastogi, S. *Macromolecules*, 47 (4), 2014: 1371-1382.

[6] Romano, D., Tops, N., Andablo-Reyes, E., Ronca, S., Rastogi, S. *Macromolecules*; 47 (14), 2014: 4750-4760.

[7] Yao, Y., Rastogi, S., Xue, H.J., Chen, Q., Graf, R., Verhoef, R. *Polymer*, 54 (1), 2013: 411-422.

[8] Ronca, S., Forte, G., Tjaden, H., Yao, Y., Rastogi, S. *Polymer*, 53, 2012: 2897-2907.

[9] Pandey, A., Champouret, Y., Rastogi, S. *Macromolecules*, 44 (12), 2011: 4952-4960.

[10] Pandey, A., Toda, A., Rastogi, S. *Macromolecules*, 44 (20), 2011: 8042-8055.

[11] Smith, P., Chanzy, H.D., Rotzinger, B.P. *Journal of Material Science*, 22, 1987: 523-531.

[12] Porter, R.S., Kanamoto, T., Zachariades, A.E. *Polymer*, 35, 23, 1994: 4979-4984.

[13] Romano, D., Ronca, S., Rastogi, S. *Macromolecular Rapid Communications*, 2014. DOI: 0.1002/marc.201400514.